



CFD-Based Analysis of Wedges Water Entry under Impact Loads

Xujian Lyu^{1*}, Dongdong Tang¹, Yanmin Guan² and Jianglong Sun³

¹School of Energy and Power Engineering, Nanjing University of Science and Technology, Nanjing 210 094, P R China

²School of Naval Architecture and Ocean Engineering, Jiangsu University of Science and Technology, Zhenjiang 212 003, P R China

³School of Naval Architecture and Ocean Engineering, Huazhong University of Science and Technology, Wuhan 430 074, P R China

Received 16 November 2018; revised 19 October 2020; accepted 03 November 2020

The impact on a falling wedge upon water entry is numerically investigated in this paper. After verified by experimental data, the numerical framework is applied for parametric studies on wedges of different drop heights and different deadrise angles to reveal the interaction behaviour between the wedge and water during impact. Pressure distribution on the wedge surface during the water entry shows that the pressure peak moves up along the surface as impact time increases. It is found that the force peak decrease with the increase of drop height and decrease of deadrise angle of the wedge. The peak positions move positively along the timeline as the increase of deadrise angle while the peak force appears just in a small impact time range for a wedge.

Keywords: CFD, Free surface, Impact, VOF, Wedge

Introduction

Since the innovative work by the pioneers, lots of studies on water impact via experiment and simulation have been proposed.^{1,2} The hydrodynamic impact is of great importance. Lots of experiments are taken to reveal the interesting interaction between structures and water during water entry.³⁻⁵ Due to the difficult of getting detailed data about pressure distribution and flow pattern in experiment, numerous numerical frameworks have been proposed to reveal the water impact phenomena. The Computational fluid dynamics (CFD) provided an opportunity to simulate complex flow problems in hydrodynamics⁶⁻⁸.

The wedge section is widely used in structure and water impact investigation because of its simple geometric and typical impact feature on water. Though a large amount of investigations have been conducted to study the water impact phenomenon^{9,10}, more clear details of the pressure and force for structures are still required for safety.^{11,12} To reveal such details, wedge sections are applied for further investigation in this paper. Calculated results including flow pattern and splash height are compared with the results from experiment by Shah *et al.*,¹³ to verify the numerical framework. The influences of impact on parameters in terms of displacement, velocity and pressure peak of the wedges are discussed to uncover the characteristics of the water entry impact.

Materials and Methods

The study addresses the models of three free falling wedges sections with different deadrise angles ($\alpha = 20^\circ$, 25° and 30°) and different falling heights ($H = 50$ mm, 100 mm and 150 mm), as shown in Fig. 1. Geometry characteristics of the physical model are performed firstly in ANSYS ICEM software, in which the flow domain, boundary definition and element meshing take place to prepare for configuration of calculation. ANSYS Fluent is used for the present simulations, where a finite volume algorithm coupled with the interface tracing method VOF is used.

For the simulations, the equation used for mass conservation is

$$\frac{\partial(\rho u_i)}{\partial x_i} = 0 \quad \dots (1)$$

The Reynolds-averaged momentum equation is

$$\begin{aligned} \frac{\partial}{\partial t}(\rho u_i) + \frac{\partial}{\partial x_i}(\rho u_i u_j) = \frac{\partial}{\partial x_j} & \\ \left[\mu \left(\frac{\partial u_i}{\partial x_j} + \frac{\partial u_j}{\partial x_i} \right) - \frac{2}{3} \mu \frac{\partial u_i}{\partial x_j} \right] - & \dots (2) \\ \frac{\partial P}{\partial x_i} + \rho g_i + F_i + \frac{\partial}{\partial x_j}(\overline{\rho u_i u_j}) & \end{aligned}$$

In these equations, u is the velocity, the subscripts i and j represent x and y components respectively; μ is the viscosity of water.

*Author for Correspondence
E-mail: xjlyu@njust.edu.cn

The VOF model for present numerical model involves an interface-tracking technique that can be applied for two or more kinds of immiscible fluid. Positions of the interface between the multiphase fluids are of interest. The model can be used for steady or unsteady tracking of any gas-liquid interface, such as present problem. Coupled with an interface compression method, this model is able to capture a sharp and clear interface with fine meshes. The volume fraction F for every mesh element is limited from 0 to 1, depending on the mixture degree relative to the reference phase. The flow properties in above equations are defined as a function of the volume fraction F as following

$$\gamma = F \cdot \gamma_{water} + (1 - F) \cdot \gamma_{air} \quad \dots (3)$$

To simulate the wedge movements, a six degree of freedom (6 DOF) solver in Fluent is applied to compute the hydrodynamic forces, acting upon the body. These forces are then used to compute the translational movements of the gravity centre of the body. The wedge is set up to move as a rigid body and Dynamic Mesh model in which meshes around moving boundaries are reconstructed is used to update the meshes of the flow domain around the body. The properties of the rigid body are set up with a user-defined function (UDF) that can be written in order to modify certain force and moment functions in Fluent. The code is written in C language and can be

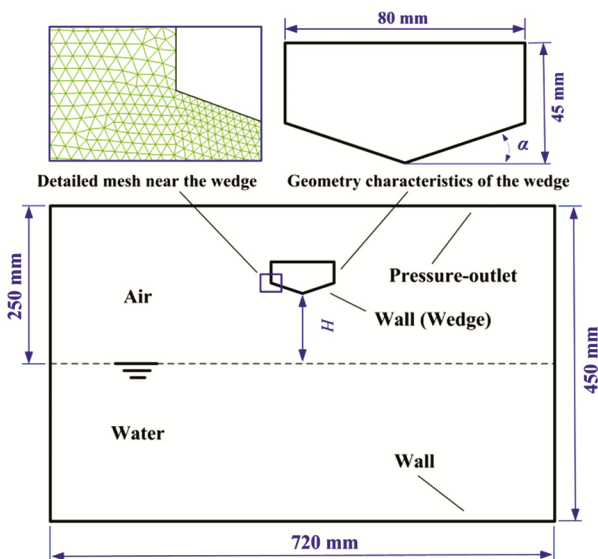


Fig. 1 — Impact pressure distribution on the wedge surface ($\alpha = 20^\circ$); The pressure peak moves up along the wedge surface as impact time increases and reaches its maximum near the end of the surface

compiled directly within Fluent. In the UDF, the wedge is defined with mass, gravity and a constant vertical drag as those in experiment. The wedge is set to move freely only in vertical direction as well.

Meshing is one of the key parts in constructing the computational model. Not only the convergence and solution accuracy but also the calculation consumption depends on the mesh quality and mesh number. The computational domain is discretised by triangular elements and mesh around the wedge body is refined for better capturing of impact phenomenon on water. Top of the computational domain is imposed of Pressure-outlet boundary condition and No-slip Wall boundary conditions are imposed at all other boundaries, including the wedge, the bottom and side wall of the computational domain, as shown in Fig. 2. Mesh dependency of the solution is studied before the hydrodynamic analysis being carried out. A mesh number of about 124 thousands is chosen finally because further refinement result in few errors for impact force.

Results and Discussion

Calculation of 9 cases is conducted for the wedge with mass of 1.6394 kg and falling mechanical drag 1.708 N, as that tested in the experiment. The gravity and falling drag based falling acceleration is 5.474 m/s^2 . With the air friction being taken into account, the monitored impact velocities for drop heights of 50 mm, 100 mm and 150 mm during the calculation are 0.721 m/s, 1.022 m/s and 1.245 m/s respectively. Physical conditions for the wedge are listed in Table 1. Results

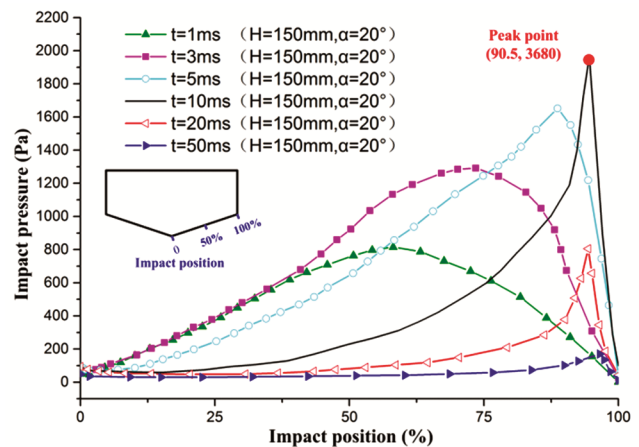


Fig. 2 — Numerical model with wedge geometry characteristics, boundary conditions and mesh details: The two-dimensional domain is defined with conditions used in Shah’s experiments¹³; Mesh around the wedge body is refined to allow better capturing of impact phenomenon on water

of present calculation and that of experiment from Shah *et al.*¹³ are compared to validate the numerical model. At the present deadrise angle range of 20°, 25° and 30°, the influences of deadrise angle α on the maximum section force F shown in calculation and experiment are not monotonic. For example, as the deadrise angle increases for the case of drop height $H = 100$ mm, the maximum impact force decreases in calculation while it decreases first and then increases in the experiment. For the one hand, there may be some errors during the experiment as discussed by Shah *et al.*¹³; for the other hand, the numerical model for present calculation is two dimensional while the experimental setup is a three dimensional one. With these factors being taken into account, the agreement between results from the calculation and the experiment is acceptable. It is found that the fluid flow patterns show excellent qualitative agreement between the results from experiment and calculation respectively as well.

During the water entry, the wedge surface should stand for temporary impact from water. To reveal the impact characteristics of the wedge during water impact, the pressure distribution along on the surface is calculated and presented in Fig 1. The horizontal coordinate axis is the concerned impact position and the vertical coordinate axis represents the impact pressure. The pressure peak moves up along the wedge surface as impact time increases. The peak value reaches maximum around 11 ms near the end of the wedge surface. This is further verified in the pressure map of flow domain around the wedge. Typical air-water flow patterns and corresponding dynamic pressure distribution around the wedge during its impact on water are depicted as well. The splash height increases as the wedge moving down into water. The maximum impact pressure for 20° wedge reaches 3680 Pa at 90.5% along the wedge surface. It is worth noting that the present maximum pressure is based on the time step $\Delta t = 0.0001$ s in the calculation, with the pressure fluctuation at high frequency that higher than 10k Hz being filtered.

Table 1 — Physical condition for the calculation cases

Drop height H (mm)	Deadrise angle α (°)	Free-fall acceleration (m/s)	Idea velocity (m/s)	Impact velocity (m/s)
50	20, 25, 30	5.474	0.740	0.721
100			1.046	1.022
150			1.281	1.245

Typical velocity and displacement of the wedge vary as a function of the falling time. As shown in Fig 3, the velocity over time is a linear function and the displacement variation over time is a quadratic one while the wedge is falling in air, before the initial point of impact. Once the impact happens, it is found that greater deadrise angle leads to more remarkable influence on movements of the wedge, i.e. the displacement and the velocity. Additional enlarged windows are used to detail the wedge’s movement in a short impact time of 40 ms. Due to inertia of the acceleration, the velocity keeps increasing slightly in the first 5 ms after the initial impact point. Subsequently, the impact results in an immediate velocity loss, i.e. 60% for the case of deadrise angle $\alpha = 20^\circ$ and 40% for the case of deadrise angle $\alpha = 30^\circ$ in 30 ms. These lead directly to the slow increase of displacement. Although it is not presented here, the variation of displacements and velocities for other cases at $H = 50$ mm and $H = 100$ mm complies with similar rules of the cases at $H = 150$ mm.

To track the impact load, the integral impact force acting on the wedge is monitored. For present cases, the integral impact forces increase first, and reach the peak values in 15~30 ms after initial point of impact. The forces fall rapidly in the next 20 ms and varies little in the next 60 ms after that as the wedge goes fully into the water. The peak values for the present cases are summarized in Table 2. It is found that the force peak decreases as the increase of drop height and decrease of deadrise angle of the wedge. The peak positions move positively along the timeline as the increase of deadrise angle. It is interesting that the

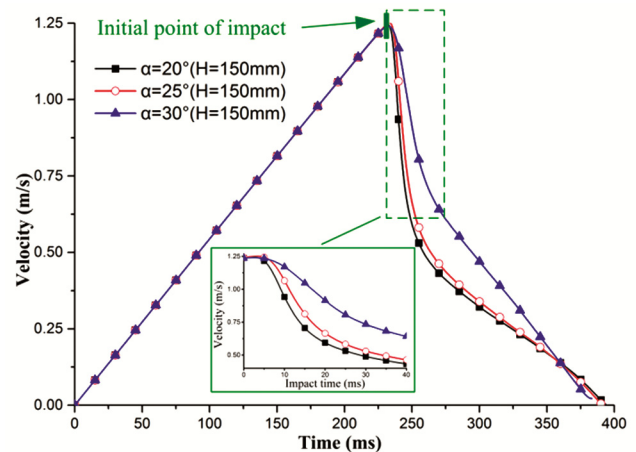


Fig 3 — Velocity of the wedge during its free falling; The velocity achieves a linear increase over time while the wedge is falling in air and decreases quickly after the impact on water

Table 2 — Peak point of the impact force acting on the wedge

Deadrise Angle (°)	Time coordinates for the peak	Peak force (N)		
		H = 50 mm	H = 100 mm	H = 150 mm
20	14.03~15.03	49.23	14.35	119.83
25	15.72~17.16	40.19	16.60	102.54
30	23.41~24.59	25.13	23.98	54.79

peak force appears in a small impact time range for a wedge, i.e. 14.03~15.06 ms for the wedge with $\alpha = 20^\circ$, 15.72~17.16 ms for the wedge with $\alpha = 25^\circ$ and 23.41~24.59 ms for the wedge with $\alpha = 30^\circ$, though the drop height varies from 50 mm to 150 mm with corresponding initial impact velocities varying from 0.721 m/s to 1.245 m/s.

Conclusions

Water entry of a wedge can be applied to model the impact phenomena for hydrodynamics structure (ship and marine structure) or navy weapons (missiles and torpedo). The present work focuses on the impact loads during water entry of a wedge, representing the impact body with three drop heights (50 mm, 100 mm and 150 mm) and three deadrise angles (20° , 25° and 30°). By the study of mesh independence and the comparison of maximum section force and the free surface evolution, the numerical framework is verified to be effective in water impact prediction for the wedge. Next, two-dimensional simulations of the model are shown in the forms of two-phase interphase and corresponding pressure distribution evolution. Impact pressure on the wedge surface during the water entry shows that the pressure peak moves up along the surface as impact time increases, and reaches its maximum (3680 Pa for present 20° wedge with drop height $H = 150$ mm) near the end of the wedge surface. Subsequent investigation shows that greater deadrise angle leads to more remarkable influence on movements of the wedge. It is found that the influence of the impact on velocity and displacement for the wedge is significant, i.e. the velocity gets immediate velocity losses of 40%~60% in a short time after the initial impact point. Finally, the integral force acting on the wedge during impact

is discussed. It is noted that the force peak decreases with the increase of drop height and the decrease of deadrise angle of the wedge respectively.

Acknowledgement

The present work is financially supported by The National Key R&D Program of China (No. 2019YFE0104800).

Reference

- Iranmanesh A, & Passandideh-Fard M, A three-dimensional numerical approach on water entry of a horizontal circular cylinder using the volume of fluid technique, *Ocean Eng* **130** (2017) 557–566.
- Nikfarjam M, Yaakob O B, Seif M S & Koto J, Investigation of wedge water-entry under symmetric impact loads by experimental tests, *Lat Am J Solids Stru*, **14** (2017) 861–873.
- Alavi Mehr J, Lavroff J, Davis M R, Holloway, D S & Thomas G A, An experimental investigation of ride control algorithms for high-speed catamarans part 2: mitigation of wave impact loads, *J Ship Res*, **61** (2017) 51–63.
- Jalalisendi M, Zhao S & Porfiri M, Shallow water entry: modeling and experiments, *J Eng Math*, **104** (2017) 131–156.
- Russo S, Biscarini C, Facci A L, Falcucci G, Jannelli E & Ubertini S, Experimental assessment of buoyant cylinder impacts through high-speed image acquisition, *J Mar Sci Tech-Japan*, **23** (2018) 67–80.
- Tu H, Yang Y, Zhang L, Xie D, Lyu X, Song L, Guan Y & Sun J, A modified admiralty coefficient for estimating power curves in EEDI calculations, *Ocean Eng*, **150** (2018) 309–317.
- Sun J, Tu H, Chen Y, Xie D & Zhou J, A study on trim optimization for a container ship based on effects due to resistance, *J Ship Res* **60** (2016) 30–47.
- Lyu X, Tu H, Xie D & Sun J, On resistance reduction of a hull by trim optimization, *Brodogradnja*, **69** (2018) 1–13.
- Lavroff J, Davis M R, Holloway D S, Thomas G A & McVicar J J, Wave impact loads on wave-piercing catamarans, *Ocean Eng* **131** (2017) 263–271.
- Kim Y, Yang K, Kim J & Zhu Z, Study of water-entry impact of wedge and ship-like section using potential theories and CFD, *Int J Offshore Polar* **27(2)** (2017) 168–176.
- Qu Q, Liu C, Liu P, Guo B & Agarwal R K, Numerical simulation of water-landing performance of a regional aircraft, *J Aircraft* **53** (2016) 1680.
- Qu Q, Hu M, Guo H, Liu P & Agarwal R K, Numerical study of ditching characteristics of a transport aircraft by global moving mesh, *J Aircraft* **52** (2015) 1550.
- Shah S A, Orifici A C & Watmuff J H, Water impact of rigid wedges in two-dimensional fluid flow, *J Appl Fluid Mech* **8** 329 (2015).